JOURNAL OF CATALYSIS 142, 381–391 (1993)

Study of Multiphasic Molybdate-Based Catalysts
II. Synergy Effect between Bismuth Molybdates and Mixed Iron and Cobalt Molybdates in Mild Oxidation of Propene

J. M. M. MILLET,* H. PONCEBLANC,*,[1] G. COUDURIER,* J. M. HERRMANN,† AND J. C. VÉDRINE*

*Institut de Recherches sur la Catalyse, CNRS, 2 Avenue Albert Einstein, 69626 Villeurbanne, France; and †Laboratoire de Photocatalyse, Catalyse et Environnement (URA CNRS 1385), Ecole Centrale de Lyon BP, 69131 Ecully, France

Received August 20, 1992; revised January 28, 1993

Results are reported concerning the synergy effect observed in the oxidation of propene to acrolein over bismuth and mixed iron and cobalt molybdates. The pure bismuth, iron, and cobalt molybdates and mixed cobalt and iron molybdates (solid solutions) have been prepared and individually tested as catalysts. Mechanical mixtures of these phases have been prepared and tested as catalysts. All the catalysts have been characterized before and after the catalytic reaction by several techniques such as ESR, XPS, EDX–STEM, TEM, XRD, and Mössbauer and UV spectroscopies. The synergy effect observed is tentatively explained as due to the deposition on the large bismuth molybdate particles of smaller mixed iron and cobalt molybdate particles with spreading of the bismuth molybdate over the latter particles. It is proposed that the $Fe_xCo_{1-x}MoO_4$ phase plays the role of the fast electron conducting material which enhances the electron mobility and the efficiency of the redox mechanism, the active and selective phase being the overlying bismuth molybdate compounds.

INTRODUCTION

In recent years many scientific investigations have been conducted on multiphasic catalysts. One reason for this is the great differences generally observed in catalytic properties between this type of catalysts, which corresponds to industrial catalysts, and single-phase catalysts. This improvement of performances for a mixture of phases with respect to each phase component, designated synergy effect, has been attributed to different effects (*1–6*). One of the most spectacular synergy effects corresponds to that observed when mixtures of bismuth molybdate and mixed iron and cobalt molybdate are used as catalysts in the oxidation of propene to acrolein. This synergy effect, which gives rise to an improvement of both the activity and the selectivity of the mixed phases, has been assigned to a support effect of the bivalent cation molybdate on the bismuth molybdate (*7*) or to a remote-control process taking place between the two different oxides (*8*) or to an interaction between phases (*9*).

EXPERIMENTAL

1. CATALYSTS PREPARATION

The bismuth molybdates $Bi_2Mo_3O_{12}$ (α-phase) and $Bi_2Mo_6O_{12}$ (γ-phase) have been prepared as follows (*10*): Molybdic acid and bismuthyl nitrate for the α-phase and ammonium heptamolybdate and bismuthyl nitrate for the γ-phase were dissolved in water and boiled under stirring. The solids were centrifuged, dried at 100°C, and calcinated at 480°C. $Bi_3FeMo_2O_{12}$, referred to as X-phase, has been prepared according to a method described by Jeitschko *et al.*

[1]Present address: Rhône–Poulenc Recherche, CRA, 52 rue La Haie Coq, 93308 Aubervilliers, France.

0021-9517/93 $5.00

(*11*). The mixed iron and cobalt molybdates $Fe_xCo_{1-x}MoO_4$ were obtained by coprecipitation, adding ammonia to an aqueous solution of $(NH_4)_6Mo_7O_{24}\cdot 4H_2O$ until pH reached 8.5. The mixture was then boiled for 2 h under argon until neutral pH was reached. A freshly prepared solution of $FeCl_2\cdot 4H_2O$ with or without $Co(NO_3)_2\cdot 6H_2O$ was added to the boiling mixture, in which argon was bubbling and then boiled for 1 h. The precipitate was filtered, washed by deoxygenated water, and then evaporated to dryness under vacuum. The ammonium metallomolybdate obtained (*12*) was calcined at 450°C for 10 h under a deoxygenated and dehydrated nitrogen flow. Mechanical mixtures were obtained by mixing and hand grinding the respective powders for 5 to 10 min.

2. Characterization

The X-ray powder diffraction patterns were recorded at room temperature with steps of 0.02°(2θ) over the angular range 10–70°(2θ) at 1 s per step, using a Siemens D500 diffractometer with Cu$K\alpha$ radiation. The chemical compositions of the pure solids and the mixtures were determined by atomic absorption and their surface area measured by nitrogen adsorption using the BET method. EDX–STEM analyses were performed with a vacuum generator VG HB 501 electron microscope with beam area varying from 0.1 μm^2 down to 5 nm^2. XPS measurements were performed on a Hewlett–Packard HP 5950. Qualitative analysis of the peaks, in terms of elemental ratios, was carried out as described previously; estimated error in such an analysis was of approximately 10% (*13*).

3. Oxidation of Propene

Selective oxidation of propene to acrolein was carried out in a conventional fixed-bed microreactor. The reactor and analysis system have been described in detail previously (*14*). Reaction conditions were as follows: propene/O_2/N_2 (diluting gas) = 1/1.69/5, total flow rate 7.2 $dm^3\ h^{-1}$, total pressure 10^5 Pa, and reaction temperature 360–450°C.

RESULTS

1. Catalytic Activity

1.1. Pure Phases

The oxidation of propene was conducted both with pure bismuth, cobalt, and iron molybdates and with different solid solutions $Fe_xCo_{(1-x)}MoO_4$. The products of the reaction were in all cases acrolein (ACRO) and CO_2. The results obtained on pure bismuth molybdates are given in Table 1; those with two polymorphic forms of the pure solid solution are given in Table 2 as a function of x.

With both bismuth molybdates, $Bi_2Mo_3O_{12}$ and Bi_2MoO_6, the acrolein selectivity is high (92%) compared to that on $Bi_3FeMo_2O_{12}$ (70%). These results are in good agreement with those obtained by Daniels and Keulks (*15*).

It is known that a polymorphic transition α/β of the mixed iron and cobalt molybdate occurs in the temperature range of the catalytic reaction (*16*) and that the high-temperature form (β) can metastably be maintained at low temperature (*17*). Consequently the solid-solution samples and the mixtures with bismuth molybdates were tested both directly after a heating to 380°C ($Fe_xCo_{(1-x)}MoO_4$ is in the α-form) and after a subsequent heating to 430°C for several hours and return to 380°C ($Fe_xCo_{(1-x)}MoO_4$ is in the β-form). The α and β solid solutions of iron and cobalt molybdates present both a very low activity and a low selectivity in acrolein compared to those obtained with bismuth molybdates (Table 1). The selectivities were also comparable and did not vary notably with the iron composition, except for the β-type solid where a small maximum was observed for x equal 0.4.

1.2. Mixtures of $Bi_2Mo_3O_{12}$ and $Fe_xCo_{(1-x)}MoO_4$

1.2.1. Influence of the iron content of the solid solution component. We have pre-

TABLE 1

Comparison of the Rate of Formation and the Selectivity in Acrolein of the Different Pure Bismuth Molybdates at 380°C

Compound	Rate of formation (10^{-8} mol. s^{-1}. m^{-2})	Selectivity (%)
Bi_2MoO_6	34	92
$Bi_2Mo_3O_{12}$	3.7	92
$Bi_3FeMo_2O_{12}$	38	70

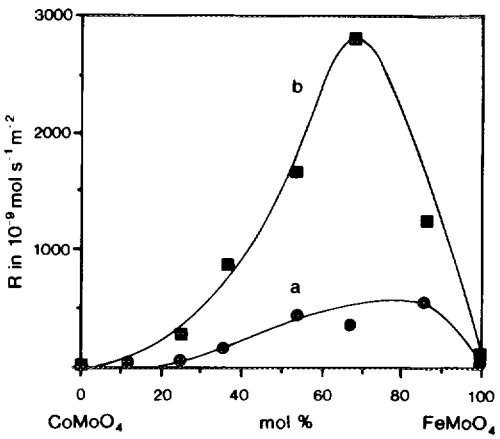

FIG. 1. Variations of the rate of formation of acrolein (R) at 380°C, on a $Bi_2Mo_3O_{12}$: $Fe_xCo_{(1-x)}MoO_4$ (0.043 : 1) catalyst, as a function of the iron molybdate content of the solid solution: (a) with α- and (b) with β-$Fe_xCo_{1-x}MoO_4$.

pared and tested mixtures of $Bi_2Mo_3O_{12}$ and $Fe_xCo_{(1-x)}MoO_4$ with a molar ratio equal to 0.043 (i.e., 15 wt%) but with different Fe contents of the solid solution. Figures 1 and 2 show the variation of the rate of formation of acrolein and of its selectivity as a function of the iron content of the solid solution. First, it can be seen that the presence of iron in the solid solution has a marked effect on both the activity and the selectivity of the catalysts. This effect was observed both for the α- and β-types but was more greatly enhanced when the solid solutions were of β-type. A maximum of activity, which corresponds to 100 times that of the β-Co MoO_4–$Bi_2Mo_3O_{12}$ mixture was observed for $x = 0.67$. The selectivity also increased with the iron content with again a larger increase observed in the case of the β-type solid solution. In the case of the α-type solid solution, the selectivity in acrolein increased regularly from 32 to 80%, reaching a maximum and then dropping to 45%. The maximum of the selectivity was observed for $x = 0.67$.

In the case of the β-type solid solution, the selectivity in acrolein increased from 54 to 91% for $x = 0.25$. It increased slightly up to 97% for $x = 0.86$ before decreasing to 40% for the $FeMoO_4$–$Bi_2Mo_3O_{12}$ mixture.

It was observed that plotting on a loga-

TABLE 2

Variation of the Rate of Formation and the Selectivity in Acrolein of the $Fe_xCo_{(1-x)}MoO_4$ Solid Solution As a Function of Its Iron Content (x)

x	With α-$Fe_xCo_{1-x}MoO_4$		With β-$Fe_xCo_{1-x}MoO_4$	
	Rate for formation (10^{-8} mol. s^{-1}. m^{-2})	Selectivity (%)	Rate of formation (10^{-8} mol. s^{-1}. m^{-2})	Selectivity (%)
0.00	0.95	25	0.95	25
0.12	1.00	25	0.80	25
0.25	1.00	28	0.80	27
0.36	3.2	29	2.1	40
0.53	2.7	27	2.1	31
0.67	2.6	22	1.8	27
0.86	1.1	17	0.95	25
1.00	0.95	18	0.6	22

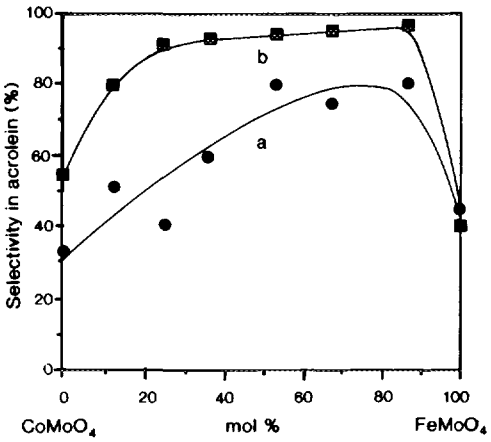

FIG. 2. Selectivity in acrolein of a $Bi_2Mo_3O_{12}$: $Fe_xCo_{(1-x)}MoO_4$ (0.043 : 1) catalyst at 380°C, as a function of the iron molybdate content of the solid solution: (a) with α- and (b) with β-$Fe_xCo_{1-x}MoO_4$.

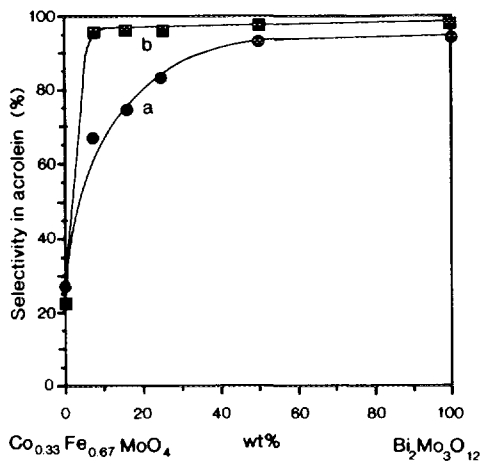

FIG. 4. Variations of the selectivity in acrolein at 380°C on $Bi_2Mo_3O_{12}$: $Fe_{0.33}Co_{0.67}MoO_4$ catalysts as a function of the $Bi_2Mo_3O_{12}$ weight content: (a) solid solution in the α-form and (b) in the β-form.

rithm scale the rate of the formation of acrolein and the electrical conductivity of the solid solution as a function of the iron atomic content of the solid solution up to 70% evidenced a rupture in slopes for both curves and this at the same iron content (17–20%) (Fig. 3). The high increase of electrical conductivity between zero and 17 at.% Fe has been attributed to a doping effect of cobalt molybdate $CoMoO_4$ by heterovalent iron ions according to the valence induction law (*20*). The similar evolution of the activity demonstrates the dependence of the catalytic properties of the mixture of molybdates phases upon the free electrons content of the solid solution.

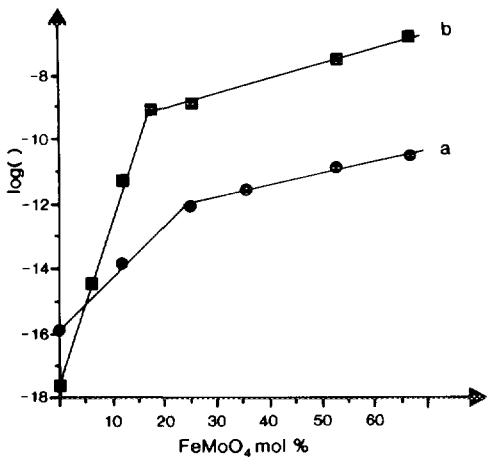

FIG. 3. Comparison of the variations (a) of the logarithm of the rate of formation of acrolein on a $Bi_2Mo_3O_{12}$: $Fe_xCo_{(1-x)}MoO_4$ (0.043 : 1) catalyst at 380°C and (b) of the logarithm of the electrical conductivity of the corresponding $Fe_xCo_{(1-x)}MoO_4$ solid solution as a function of its iron molybdates content.

1.2.2. Influence of the bismuth molybdate content of the mixtures. Four mixtures composed of $Bi_2Mo_3O_{12}$ and a mixed iron and cobalt molybdate with the composition $Fe_{0.67}Co_{0.33}MoO_4$ were prepared. The weight contents in $Bi_2Mo_3O_{12}$ of these mixtures were equal to 7, 15, 25, and 50% (i.e., 1.8, 4.3, 7.4, and 19.3 mol%). The rates of formation of acrolein and the selectivity in acrolein observed at 380°C on these catalysts as a function of their bismuth molybdate content are presented respectively in Fig. 4 and 5. The results, gathered in Table 3, show that the activity and the selectivity of the catalysts increased with the bismuth molybdate content. The activity increased slowly to reach a maximum for a weight content of bismuth molybdate of 50% when the solid solution is in the α-form, whereas it

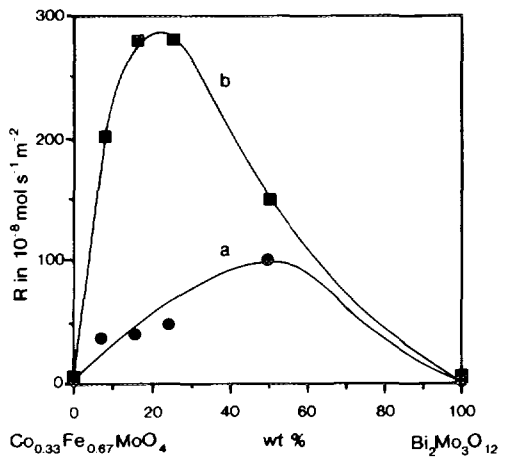

FIG. 5. Variations of rate of formation of acrolein at 380°C on $Bi_2Mo_3O_{12}$: $Fe_{0.33}Co_{0.67}MoO_4$ catalysts as a function of the $Bi_2Mo_3O_{12}$ weight content: (a) solid solution in the α-form and (b) in the β-form.

increased sharply to a maximum for a mass content of bismuth molybdate of 20% when it is in the β-form. Such maximum was three times higher with a β-type solid solution than with an α-type.

1.2.3. Influence of the nature of the bismuth molybdate. Mixtures of Bi_2MoO_6, $Bi_2Mo_3O_{12}$, or $Bi_3FeMo_2O_{12}$ with a solid solution of composition $Fe_{0.25}Co_{0.75}MoO_4$ have been prepared and run as catalyst. The composition of the mixtures approximated $BiCo_8Fe_{2.5}Mo_{12}O_{48}$, corresponding respectively to 14.7 wt% Bi_2MoO_6, 20.7 wt% $Bi_2Mo_3O_{12}$, and 17.0 wt% $Bi_3FeMo_2O_{12}$. The results obtained are compared to the theoretical values calculated from the activities and the selectivities of the pure phases and of the solid solution assuming that they are additive properties (Table 4). It can be seen, as previously, that the activities are much higher than the theoretical values by a factor 10 to 20 for the solid solution in the α-form, and 100 in the β-form. The selectivities are also strongly enhanced up to 98%, particularly for the solid solution in its β-form. The three bismuth molybdates have comparable activities and selectivities that points out that the synergy effect depends more on the characteristics of the solid solution than on those of the bismuth molybdate.

1.3. Mixtures of $Bi_2Mo_3O_{12}$, $FeMoO_4$, and $CoMoO_4$

A three phase mechanical mixture containing $Bi_2Mo_3O_{12}$, β-$FeMoO_4$, and β-$CoMoO_4$ were also prepared. The relative proportion of the phases used to prepare this mixture were chosen in order to correspond to the composition of the mechanical mixture of $Bi_2Mo_3O_{12}$ and $Fe_{0.12}Co_{0.88}MoO_4$ with 25 wt% of the first phase (i.e., 7.4 mol%). The catalytic performances of this ternary mixture are compared, in Table 5, to those of binary mixtures and of a coprecipitate

TABLE 3

Activities and Selectivities in Acrolein of the Mechanical Mixtures of $Bi_2Mo_3O_{12}$ and $Fe_{0.67}Co_{0.33}MoO_4$ at 380°C

weight% of $Bi_2Mo_3O_{12}$	S_{BET} ($m^2 \cdot g^{-1}$)	With α-$Fe_{0.67}Co_{0.33}MoO_4$		With β-$Fe_{0.67}Co_{0.33}MoO_4$	
		Rate of formation (10^{-8} mol. s^{-1}. m^{-2})	Selectivity (%)	Rate of formation (10^{-8} mol. s^{-1}. m^{-2})	Selectivity (%)
0	17	2.6	22	1.8	27
7	13	37	67	200	96
15	9	41	75	280	96
25	10	49	83	280	96
50	9	100	94	150	98
100	0.3	3.7	94	3.7	98

Note. S_{BET}: specific surface area.

TABLE 4

Rate of Formation and Selectivity in Acrolein of the Mechanical Mixtures of Bismuth Molybdates and $Fe_{0.25}Co_{0.75}MoO_4$ in the Partial Oxidation of Propene at 380°C

Bismuth molybdate	S_{BET} ($m^2 . g^{-1}$)	With α-$Fe_{0.67}Co_{0.33}MoO_4$		With β-$Fe_{0.67}Co_{0.33}MoO_4$	
		Rate of formation (10^{-8} mol. s^{-1}. m^{-2})	Selectivity (%)	Rate of formation (10^{-8} mol. s^{-1}. m^{-2})	Selectivity (%)
Bi_2MoO_6	18	29	61	100	89
$Bi_2Mo_3O_{12}$	19	13	54	57	91
$Bi_3FeMo_2O_{12}$	23	15	45	110	92
		Theoretical values			
Bi_2MoO_6		1.3	24	1.1	24
$Bi_2Mo_3O_{12}$		0.7	41	0.6	24
$Bi_3FeMo_2O_{12}$		1.1	23	1.0	23

Note. S_{BET}: specific surface area.

of similar composition. The ternary mixture was a little less selective in acrolein but much more active than the pure $Bi_2Mo_3O_{12}$ sample (see Table 1) and the results obtained were actually intermediate between those obtained with the two-phase mixtures. Note also that the values of activity and selectivity are much higher than the theoretical ones.

The characterization of the catalysts after catalysis showed that the cobalt and the iron molybdates had not reacted to form the solid solution (*18*), which consequently shows that the synergy effect can take place with the pure molybdates and does not depend only on the formation of the solid solution. Comparison with the coprecipitate evidences that the contact between the phases is a very important factor.

2. Characterization of the Catalysts

2.1. XRD, BET Surface Area, and Chemical Analysis

XRD analyses of the solid solution compounds have been described previously (*17*). The analysis of the mixture before and after catalysis only showed the α/β transformation of the mixed iron and cobalt molyb-

TABLE 5

Activities and Selectivities in Acrolein of Ternary and Binary Mixtures Containing 25 wt% of $Bi_2Mo_3O_{12}$ and Co, Fe Molybdates in the β-Form

Composition of Co, Fe molybdates	Rate of formation (10^{-8} mol. s^{-1}. m^{-2})	Selectivity (%)
$0.12FeMoO_4 + 0.88CoMoO_4$	17	90
$Fe_{0.12}Co_{0.88}MoO_4$	5.8	80
$Fe_{0.25}Co_{0.75}MoO_4$	30	91
Coprecipitate[a]	84	97
Theoretical values	0.3	42

[a] Coprecipitate with the similar composition was prepared according to the "coevaporated mixtures method" (*9*) by evaporating an aqueous slurry containing all the elements, drying and calcining.

TABLE 6

Atomic Compositions Determined by Chemical Analysis and Surface Areas of the Compounds, Calcined at 450°C

Compound	S_{BET} ($m^2 . g^{-1}$)	$Fe_t/(Fe_t + Co)$	$(Co + Fe_t)/Mo$
$CoMoO_4$	5	0	0.97
$Co_{0.88}Fe_{0.12}MoO_4$	16	0.06	0.93
$Co_{0.75}Fe_{0.25}MoO_4$	17	0.11	0.93
$Co_{0.64}Fe_{0.36}MoO_4$	13	0.12	0.90
$Co_{0.47}Fe_{0.53}MoO_4$	13	0.17	0.96
$Co_{0.33}Fe_{0.67}MoO_4$	17	0.23	0.98
$Co_{0.14}Fe_{0.86}MoO_4$	17	0.25	0.92
$FeMoO_4$	22	0	0.97
Compound	S_{BET} ($m^2 . g^{-1}$)	Fe/Bi	Bi/Mo
$Bi_2Mo_3O_{12}$	0.3	—	0.7
Bi_2MoO_6	1.7	—	2.03
$Bi_3FeMo_2O_{12}$	1.8	0.67	1.53

Note. $Fe_t = Fe^{2+} + Fe^{3+}$.

dates. No phase susceptible to appear in the conditions of the catalysis reaction were detected. This was confirmed by IR spectroscopy and ESR since no new ferric species were detected (*18*). The results obtained in the surface area determinations and the chemical analyses are presented in Table 6. All values of the surface areas were comprised between 10 and 20 $m^2 g^{-1}$ except for $Bi_2Mo_3O_{12}$ and $Bi_3FeMo_2O_{12}$ which exhibit low surface areas of the order of 1 $m^2 . g^{-1}$. It has been controlled that after catalysis the surface area of the various samples did not change significantly. The chemical analyses are in relatively good agreement with the theoretical stoichiometries.

2.2. EDX–STEM

The analysis by EDX-STEM has been focused on a $Bi_2Mo_3O_{12}$–$Fe_{0.67}Co_{0.33}MoO_4$ mixture containing 15 wt% $Bi_2Mo_3O_{12}$ (*18, 21, 22*). Two distinct sets of particles have been observed before catalysis. The first particles set with a size of 0.1 to 0.2 μm only contained mixed iron and cobalt molybdates with an Fe/(Fe + Co) atomic ratio calculated from 16 individual analyses equal to 0.64 ($\pm$0.03). The second particle type with a larger size (1 to 3 μm) contained only the bismuth molybdates; no cobalt or iron was detected in the analyses.

After catalysis, the two types of particles were always present. The smaller particles which had the same size were either isolated (with exactly the same composition as before catalysis where no bismuth was detected) or stuck around the larger particles which had a size slightly reduced (0.7 to 2.5 μm). These larger particles appeared then to be composed of bismuth and molybdenum and also of cobalt and iron in variable contents but in the same Fe/(Fe + Co) atomic ratio as in the small isolated particles. Such detection was independent of the size of the analyzed area (from 5 nm^2 to 1μm^2). This shows that during catalysis a change in morphology occurs with a sticking of a part of the solid solution particles on the large bismuth molybdate particles.

2.3. XPS Analysis

XPS technique was used to characterize three samples of $Bi_2Mo_3O_{12}$–$Fe_{0.67}Co_{0.33}$

TABLE 7

Comparison of the Surface Elementary Ratios of the Cations in the Mechanical Mixtures of $Bi_2Mo_3O_{12}$ and $Fe_{0.67}Co_{0.33}MoO_4$ Calculated from XPS Analysis Data before and after Catalytic Reaction and Those Calculated from Chemical Analysis Data before Catalysis

Weight % of $Bi_2Mo_3O_{12}$		Mo/O	(Fe + Co)/$\Sigma_{cat.}$	Bi/$\Sigma_{cat.}$	Mo/$\Sigma_{cat.}$	Bi/(Fe + Co)	Fe/(Fe + Co)
7	Before catalysis	0.26	0.45	0.0018	0.55	0.0039	0.60
	After catalysis	0.25	0.41	0.036	0.56	0.089	0.63
	Chemical analysis	0.25	0.48	0.018	0.51	0.038	0.67
25	Before catalysis	0.25	0.44	0.012	0.55	0.03	0.57
	After catalysis	0.25	0.36	0.062	0.58	0.17	0.48
	Chemical analysis	0.25	0.41	0.067	0.52	0.16	0.67
50	Before catalysis	0.25	0.44	0.056	0.50	0.14	0.72
	After catalysis	0.26	0.38	0.082	0.54	0.22	0.63
	Chemical analysis	0.25	0.31	0.15	0.54	0.49	0.67

Note. $\Sigma_{cat.}$: sum of all the cations.

MoO_4 mixtures containing respectively 7, 25, and 50 wt% of $Bi_2Mo_3O_{12}$. Characterization was carried out before and after catalytic reaction, Bi, Mo, Fe, Co, and O being analyzed. The results obtained are presented in Table 7. It is worth noting that if the Mo/O ratio remained equal to 0.25 for all the samples, before and after catalysis, the Bi/(Fe + Co) ratio increased systematically. It can be observed that before catalysis this ratio was always lower than that calculated from chemical analysis. This can be explained by the difference of a factor of 10 between the particle size of the bismuth molybdate and the iron and cobalt molybdates, the surface contribution being about 10 times less for the bismuth molybdate than for the other molybdate since the sizes of the corresponding particles are in an inverse ratio.

After catalysis, the Mo/$\Sigma_{cat.}$ ratio remained constant whilst the Bi/(Fe + Co) ratio increased in a factor 20, 6, and 2, respectively. This increase could be explained by the decrease in size of the bismuth molybdate particles but the variations observed by electron microscopy are too weak to account for this observation. In agreement with the EDX–STEM observations, the covering of the bismuth molybdate particles by the iron and cobalt molybdate particles during catalysis should lead to a decrease of this ratio. Therefore, one may suggest that part of bismuth molybdate migrates on the surface of the particles of the solid solution stuck on the bismuth molybdate. The migration of the only bismuth element may be ruled out because the Bi/(Fe + Co) ratio should then be much higher and the Mo/$\Sigma_{cat.}$ ratio should be smaller, in contrast with the experimental results.

DISCUSSION

The above catalytic activity results show that a synergy effect takes place between a bismuth molybdate and a mixed iron and cobalt molybdate whatever the bismuth molybdate phase is.

Among the parameters influencing the synergy effect, the most important appeared to be the iron content of the solid solution and the bismuth molybdate content, in a lesser extent. This effect is much higher for the solid solution in β-form rather than in α-form.

We have shown that the iron content had a rather limited influence on the unit cell parameters and on the morphology of the solid solution (*16*). This tends to rule out the explanation of the synergy effect based in

the first case only on a crystallographic fit between the two molybdates (*23*) and in the second case on a reaction mechanism with reaction steps occurring on different phases. Furthermore, it has been shown that similar synergy effect was observed with different bismuth molybdates and with coprecipitate. It is worth noting that if $Bi_2Mo_3O_{12}$ is supported on $Co_{11/12}Fe_{1/12}MoO_x$ (*7*), the catalytic performances measured at 450°C increase with the bismuth molybdate content up to 30 wt%. We do observe the same trend at 380°C. This phenomenon was attributed to a strong interaction between $Bi_2Mo_3O_{12}$ and the support which acts as a "water tank" (*7*).

From our results, the catalytic synergy that actually implies an interaction between the molybdates may be better explained on the basis of both an electronic effect and an evolution of the morphology related to the spreading of part of the bismuth molybdate.

1. Electronic Effect of the Mixed Iron and Cobalt Molybdate

The comparison of the variation of the electric conductivity and of the rate of formation of acrolein as a function of the iron content of the mixed iron and cobalt molybdates (Fig. 3) allow us to conclude that the rate of formation of acrolein at 380°C follows quite well the electric conductivity of this component in the catalyst. This demonstrates the importance of the electronic exchange between the two phases on the catalytic properties. The electrons stemming from the oxidation of the propene molecule on the bismuth molybdate are easily transferred to the highly conductive solid solution which should play an important role in the redox mechanism. These electronic exchanges are facilitated by the presence in the solid solution of Fe^{3+} species giving rise to a valence induction, as shown previously (*19*, *20*). Such a transfer of the electrons stemming from the reactant to the solid solution (as free electrons) does not require a simultaneous loss of oxygen anions. The other factor which will influence the transfers will be the quality of the contact between the two (or the three) phases and we have shown that such intimate contacts were developed in the conditions of the catalytic reaction or were preexisting in the coprecipitate catalyst.

The fact that oxygens of the solid solution could be involved in the catalytic reaction has been shown (*7*, *24*) and may correspond to a remote control mechanism for oxygen ions transfer but no attempt to demonstrate it has been performed in this work.

2. Evolution of the Morphology of the Catalysts during the Reaction

The bulk analysis by XDR, IR, or ESR of the catalysts after catalysis did not show the formation of any new phase. The surface analysis tends also to show that no new phase was formed at the surface since the Mo/O ratio at the surface remained exactly the same after catalysis (Table 7). The molybdates susceptible to be formed should present a much lower Mo/O ratio (0.17 for Bi_2MoO_6 and $Bi_3FeMo_2O_{12}$). Concerning the Bi/(Fe + Co) ratio, it can first be observed that before catalysis this ratio was always lower than that calculated from chemical analysis. This was explained by the difference between the particles size of the bismuth molybdate and the iron and cobalt molybdates. Second, the Bi/(Fe + Co) ratio increased systematically after catalysis which was explained by the covering of the iron and cobalt molybdate particles by the bismuth molybdate.

Before catalysis the particles of the bismuth molybdate and of the solid solution are separated. After catalysis, the large particles of bismuth molybdates are covered by a number of small particles of solid solution as it was shown by EDX–STEM. These small particles are themselves covered by bismuth molybdate since the Bi/(Fe + Co), observed by XPS, increased instead of decreasing after catalysis. It can be seen that this ratio becomes for certain catalysts even larger than the chemical ratio (Table 7). Such a phenomenon can only be explained

by the covering of the solid solution by the bismuth molybdate.

The spreading of the bismuth molybdate on the solid solution should take place at around 400°C under catalytic reaction conditions. In these conditions, the α/β phase transition also occurred. We may conclude that the observed activation is due to both transformations.

The maximum of activity observed around 20 wt% $Bi_2Mo_3O_{12}$ with $Fe_{0.67}Co_{0.33}MoO_4$ may correspond to the maximum coverage of the bismuth molybdate by the solid solution particles. The difference of the maximum between the α- and β-phase could be explained by the fact that the spreading may occur more easily on the β-phase, but here again it is difficult to determine if it is the type of polymorph or the heat treatment which is related to this phenomenon.

The observation of a synergy effect with a ternary phase mixture $Bi_2Mo_3O_{12}$–$CoMoO_4$–$FeMoO_4$ tends to show that the properties of the solid solution are not the only major factor influencing the synergy effect. Furthermore we have shown that the same type of morphology evolution was taking place in this case as in the case of mixtures of $Bi_2Mo_3O_{12}$ and solid solution samples (*18*).

The spreading of $Bi_2Mo_3O_{12}$ on $Fe_xCo_{(1-x)}MoO_4$ can be related to the wetting of an oxide by another as observed in the case of V_2O_5 on TiO_2 (*25*) and $NiMoO_4$ on $MgMoO_4$ (*26*). These transformations are generally difficult to characterize since they can occur only partly and cannot be practically detected by direct observation of the solids. Theoretical approach has been proposed by Stoneham *et al.* (*27*).

CONCLUSIONS

The general conclusions drawn from our results are that the ability for the bismuth and cobalt–iron molybdates particles to exchange electrons and oxygen anions and the change of morphology of the catalyst under the conditions of the catalytic reaction with spreading of the oxides one over the other are both to be considered to explain the synergy effect in molybdate-based catalysts. The first phenomenon which is enhanced by the high electrical conductivity of the cobalt–iron molybdate, related to Fe^{3+} species giving rise to a valence induction effect, should be very dependent on the change in morphology which, with the formation of intimate contacts between bismuth molybdate and solid solution, facilitates electrons and oxygen ions mobility from one phase to the other. This type of change in morphology should be systematically searched for when synergy effects between simple mechanical mixtures of phases are observed.

REFERENCES

1. Carson, D., Coudurier, G., Forissier, M., and Védrine, J. C., *J. Chem. Soc. Faraday Trans. I* **79,** 1921 (1983).
2. El Jamal, M., Forissier, M., Coudurier, G., and Védrine, J. C., *in* "Proceedings, 9th International Congress on Catalysis" (M. J. Phillips and M. Ternan, Eds.), p. 1617. Chem. Institute of Canada, Ottawa, 1988.
3. Ruiz, P., Zhou, B., Rémy, M., Machej, T., Aoun, F., Doumain, B., and Delmon, B., *Catal. Today* **1,** 181 (1987).
4. Ceckiewicz, S., and Delmon, B., *Bull. Soc. Chim. Belg.* **93,** 163 (1984).
5. Meriaudeau, P., and Védrine, J. C., *Nouv. J. Chim.* **2,** 133 (1978).
6. Védrine, J. C., Praliaud, H., Mériaudeau, P., and Che, M., *Surf. Sci.* **80,** 101 (1979).
7. Moro-Oka, Y., He, D. H., and Ueda, W., *in* "Structure–Activity Relationships in Heterogeneous Catalysis" (R. K. Grasselli and A. W. Sleight, Eds.), Studies in Surface Science and Catalysis, Vol. 67, p. 57. Elsevier, Amsterdam, 1991.
8. We, L. T., and Delmon, B., *Appl. Catal. A* **81,** 141 (1992).
9. Legendre, O., Jaeger, Ph., and Brunelle J. P., *in* "New Developments in Selective Oxidation by Heterogeneous Catalysis" (P. Ruiz and B. Delmon, Eds.), Studies in Surface Science and Catalysis, Vol. 72, p. 387. Elsevier, Amsterdam, 1992.
10. Batist, P. A., *J. Chem. Tech. Biotechn.* **29,** 451 (1979).
11. Jeitschko, W., Sleight, A. W., McCellan, W. R., and Weiher, J. F., *Acta Crystallogr.* **32,** 1163 (1976).
12. Pezerat, H., *C. R. Acad. Sci. Paris* **26,** 5490 (1965).
13. Védrine, J. C., and Jugnet, Y., *in* "Les techniques physiques d'étude des catalyseurs" (B. Imelik and J. C. Védrine, Eds.), p. 365. Technip, Paris, 1988.
14. Forissier, M., Larchier, A., Demourgues, L., Perrin, M., and Portefaix, J. L., *Rev. Phys. Appl.* **11,** 639 (1976).

15. Daniels, C., and Keulks, G. W., *J. Catal.* **29,** 475 (1973).
16. Sleight, A. W., and Chamberland, B. L., *Inorg. Chem.* **7,** 1672 (1968).
17. Ponceblanc, H., Millet, J. M. M., Coudurier, G., Legendre, O., and Védrine, J. C., *J. Phys. Chem.* **96,** 9462 (1992).
18. Ponceblanc, H., Thesis, Lyon, France, No. 259-90, 1990.
19. Ponceblanc, H., Millet, J. M. M., Thomas, G., and Védrine, J. C., *J. Phys. Chem.* **94,** 9466 (1992).
20. Ponceblanc H., Millet, J. M. M., Coudurier, G., Herrmann, J. M., and Védrine, J. C., *J. Catal.*, **143,** 373 (1993).
21. Ponceblanc H., Millet, J. M. M., Coudurier, G., and Védrine, J. C., *Prepr.–Am. Chem. Soc. Div. Pet. Chem.* **37,** 1114 (1992).
22. Ponceblanc, H., Millet, J. M. M., Coudurier, G., and Védrine, J. C., *in* "Catalytic Selective Oxidation" (S. T. Oyama and J. W. Hightower, Eds.), Am. Chem. Soc. Symposium Series, Washington, DC, in press.
23. Brazdil, J. F., Mehiric, M., Glaeser, L. C., Hazle, M. A. S., and Grasselli, R. K., "Catalyst Characterization Science." p. 26. 1985.
24. Ueda, W., Moro-Oka, Y., Ikawa, T., and Matsuura, I., *Chem. Lett.*, 1365 (1982).
25. Courtine, P., and Véjux, A., *C. R. Acad. Sci. Paris* **286,** 135 (1978).
26. Haber, J., Mielczarska, E., and Turek, W., *Z. Phys. Chem. Neue Folge* **144,** 69 (1985).
27. Stoneham, A. M., and Tasker, P. W., *Philos. Mag. B* **55,** 237 (1987) and *in* "Ceramic Microstructures" (J. A. Pask and A. G. Evans, Eds.) p. 155, Plenum Pub. Corp., New York 1987.